

Electronic structure of the SrTiO₃/LaAlO₃ interface revealed by resonant soft x-ray scattering

H. Wadati,¹ D. G. Hawthorn,¹ J. Geck,¹ T. Higuchi,² Y. Hikita,² H. Y. Hwang,^{2,3} S.-W. Huang,⁴ D. J. Huang,⁴ H.-J. Lin,⁴ C. Schuler-Langeheine,⁵ H.-H. Wu,^{4,5} E. Schierle,⁶ E. Weschke,⁶ and G. A. Sawatzky¹

¹Department of Physics and Astronomy, University of British Columbia, Vancouver, British Columbia V6T 1Z1, Canada

²Department of Advanced Materials Science, University of Tokyo, Kashiwa, Chiba 277-8561, Japan

³Japan Science and Technology Agency, Kawaguchi 332-0012, Japan

⁴National Synchrotron Radiation Research Center, Hsinchu 30076, Taiwan

⁵II. Physikalisches Institut, Universität zu Köln, Zulpicher Straße 77, D-50937 Köln, Germany

⁶Heinrich-Zentrum Berlin für Materialien und Energie c/o BESSY, Albert-Einstein-Str. 15, D-12489 Berlin, Germany

(Dated: February 20, 2024)

We investigated the electronic structure of the SrTiO₃/LaAlO₃ superlattice (SL) by resonant soft x-ray scattering. The (003) peak, which is forbidden for our "ideal" SL structure, was observed at all photon energies, indicating reconstruction at the interface. From the peak position analyses taking into account the effects of refraction, we obtained evidence for electronic reconstruction of Ti 3d and O 2p states at the interface. From reactivity analyses, we concluded that the AlO₂/LaO/TiO₂/SrO and the TiO₂/SrO/AlO₂/LaO interfaces are quite different, leading to highly asymmetric properties.

PACS numbers: 73.20.-r, 78.70.Ck, 71.28.+d, 73.61.-r

Many oxide hetero-epitaxial devices confront the need to manage different possible interface atomic configurations, which can have important effects on the electronic structure at the most electrically sensitive regions of the device. For example, in (001) oriented manganite tunnel junctions or cuprate Josephson junctions, a perovskite such as SrTiO₃ (STO) is typically used as the insulating barrier. Because perovskites grow in unit cell blocks (a SrO/TiO₂ double layer for STO) in most growth techniques, the top and bottom interfaces across the barrier have different atomic terminations. Although most studies assume a symmetric barrier in these junctions neglecting this interface asymmetry, evidence is emerging that this is a crucial issue to understand and optimize [1].

One example of extremely anisotropic properties that arise as a function of interface termination is the interface between two band insulators STO and LaAlO₃ (LAO). This system is especially interesting due to the metallic conductivity [2] and even superconductivity [3] found at the interface. The electronic structure of this interface has been studied both experimentally [4, 5, 6, 7, 8, 9, 10, 11] and theoretically [12, 13], and there has been an intense debate about the origin of this metallicity, that is, whether it is due to oxygen vacancies ("extrinsic") [9, 10] or due to the polar nature of the LAO structure [4], which could result in "electronic reconstruction" as found in surfaces of polar materials by Hesper et al [14]. Photoemission spectroscopy has been recently used to observe the electronic structures of such interfaces directly [15, 16, 17, 18], but it cannot be applied to the study of multilayers with several periods due to its surface sensitivity.

In this study we investigated the electronic structure of the STO/LAO superlattice (SL) by resonant

soft x-ray scattering [19], which has recently been used to study LaMnO₃ (LMO)/SrMnO₃ (SMO) [20] and La₂CuO₄/La_{1.64}Sr_{0.36}CuO₄ [21] SLs. Since x-ray scattering is a photon-in-photon-out process, resonant soft x-ray scattering is bulk-sensitive, and can be applied to insulators as well as metals. In this sense, this technique is complementary to photoemission, and well suited for studying the electronic structure of multilayers non-destructively. The (003) forbidden peak was used in Ref. [20] to study the electronic structure of symmetric interfaces in LMO/SMO. Here we show that a similar experimental approach can be used to differentially probe the asymmetry of interfaces in ABO₃/A⁰B⁰O₃ SLs, where two distinctly different interfaces are formed. We introduce a model which is used to analyze the energy dependence of the scattering in terms of the known energy dependence of the absorption of the parent bulk compounds, by taking into account the effects of the photon energy dependent refraction, the finite thickness of the SL, which removes the total extinction in otherwise forbidden (003) reflections, and the photon energy dependent absorption depth which again has an energy dependent finite size effect. From our study of the photon-energy-dependent (002) and (003) Bragg peak positions and the overall reactivity spectra, we obtained evidence for electronic reconstruction and strong asymmetric properties at the two different STO/LAO interfaces.

The SL sample consisted of seven periods of 12 unit cells (uc) of STO and 6 uc of LAO. A schematic view of the fabricated SL is shown in Fig. 1 (c). The present samples were grown on a TiO₂-terminated STO (001) substrate [22] by pulsed laser deposition at an oxygen pressure of 1.0 × 10⁻⁵ Torr and a substrate tempera-

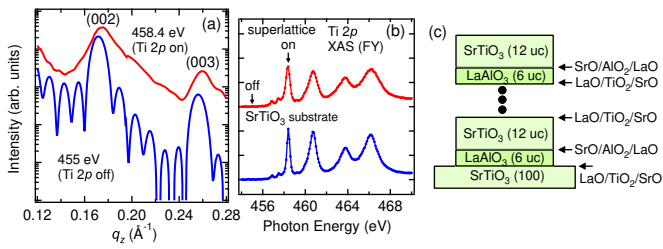


FIG. 1: (Color online) X-ray reflectivity and absorption spectra from the SrTiO₃/LaAlO₃ superlattice. (a) Reflectivity spectra measured at 458.4 eV (Ti 2p on-resonance) and 455 eV (Ti 2p off-resonance). (b) Ti 2p absorption spectra. (c) Schematic view of the SrTiO₃/LaAlO₃ superlattice.

ture of 1073 K. The lattice constant of one period of the SL was determined to be 73.45 Å. The resonant soft x-ray scattering experiments were performed at the EPU beam line of NSRRC, Taiwan. The spectra were taken at 80 K. The incident light was polarized in the scattering plane (p-polarization) with the detector integrating over both normal polarizations, i.e., both the σ and π scattering channels. We also measured x-ray absorption spectroscopy (XAS) spectra in the fluorescence yield (FY) mode.

Figure 1 shows the x-ray reflectivity (a) and absorption (b) spectra measured in the energy region of Ti 2p absorption. Figure 1 (b) shows that the XAS spectrum of the SL sample is almost the same as that of the STO substrate, which means that the formal valence of Ti is close to 4+ in the SL. The reflectivity spectra in Fig. 1 (a) show finite-size Fresnel oscillations from the SL structures, and (002), and (003) Bragg peaks. The oscillations are clear at 455 eV (Ti 2p off-resonance), but not evident at 458.4 eV (Ti 2p on-resonance). This is because the attenuation length of photons at 455 eV is about 100 nm, which covers seven periods in the SL, but at 458.4 eV it is only about 20 nm [23], which covers only three periods. Since the ratio of STO and LAO thicknesses are 2:1, the (003) peak is forbidden in infinitely thick and the zero absorption limit for samples of the ideal structure, just as in the case of the LMO/SMO SL studied in Ref. [20]. In the case of LMO/SMO SL, the (003) peak was observed only on-resonance, but here it is observed in both on- and off-resonance. This is due to the strong asymmetry of the present SL, which contains two types of interfaces, the AlO₂/LaO/TiO₂/SrO and the TiO₂/SrO/AlO₂/LaO interfaces, as shown in Fig. 1 (c). In the LMO/SMO SL, there is only one kind of interface (SrO/MnO₂/LaO) because both LMO and SMO have MnO₂ layers. We now focus on (002), which is a normal Bragg peak, and (003), a forbidden interface-sensitive peak.

Figure 2 shows the photon-energy dependence of the (002) and (003) peaks near the Ti 2p (a) and O 1s (b) absorption edges. From the top and middle panels one can

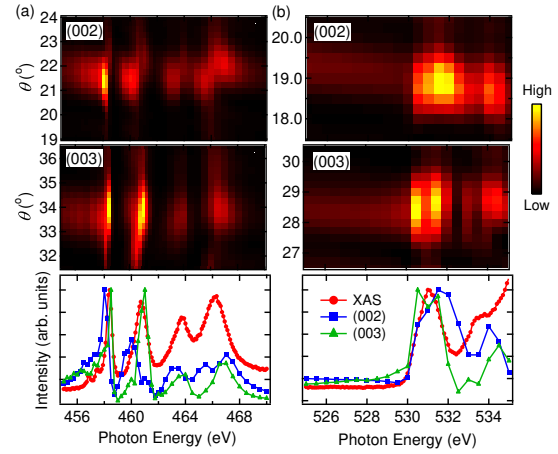


FIG. 2: (Color online) Photon-energy dependence of the (002) and (003) peaks near the Ti 2p (a) and O 1s (b) absorption edges. Top and middle panels show intensity maps of (002) and (003) regions, respectively. Here bright parts correspond to high intensities. Bottom panels show the (002) and (003) peak heights together with the XAS spectra.

see that both the (002) and (003) peaks show resonant enhancement at these edges. The bottom panels show the (002) and (003) peak heights together with the XAS spectra. These peaks show enhancement where the Ti 2p or O 1s absorption is strong. In O 1s there is no evidence of pre-edge structures from states in the band gap. This is in sharp contrast to the results of the LMO/SMO SL [20], where a pre-edge feature appears corresponding to states at the Fermi level. This difference can be explained by the difference of the mechanism of metallicity. In the case of LMO/SMO, metallic behavior is due to the hole-doping of insulating LMO, resulting in unoccupied states at the top of the valence band, whereas in the case of STO/LAO, metallicity is due to electron-doping of insulating STO so no new unoccupied states appear that would be probed by resonant soft x-ray scattering. We should note here that the energy-dependent behaviors of the (002) and (003) peaks are different, indicating a difference in the states at the interface from the bulk.

We now analyze the peak positions in these absorption edges. In the normal Bragg's law $m\lambda = 2d \sin \theta$, where m is an integer, and d is the thickness of one unit cell of the SL. However, near the absorption edges, we must use the following modified Bragg's law [24], which takes into account the effects of refraction:

$$m\lambda = 2d \sin \theta \sqrt{1 - \frac{4\alpha^2}{m^2 \lambda^2}} \quad (1)$$

Here the refractive index n is written as $n = 1 - \alpha + i\beta$. For a system with ideally sharp interfaces between the two components, α is defined as the average of α 's of STO

and LAO .

$$= \frac{d_{\text{STO}} d_{\text{STO}} + d_{\text{STO}} d_{\text{LAO}}}{d_{\text{STO}} + d_{\text{LAO}}}, \frac{2 d_{\text{STO}} + d_{\text{LAO}}}{3}; \quad (2)$$

where d_{STO} and d_{LAO} are the thickness of STO and LAO in one SL unit cell ($d = d_{\text{STO}} + d_{\text{LAO}}$). and are related to the real and imaginary parts of the atomic scattering factors f_1^0 and f_2^0 , respectively. The relationships are

$$= \frac{n_a r_e^2}{2} f_1^0; \quad = \frac{n_a r_e^2}{2} f_2^0; \quad (3)$$

where n_a is density of atoms and r_e is the classical electron radius. Since f_1^0 cannot be determined experimentally, we use the relationship that f_2^0 is proportional to absorption and determined f_2^0 from the XAS spectra normalized to the values from Henke's table [25]. f_1^0 is then obtained from the following Kramers-Kronig transformation

$$f_1^0(\omega) = Z \int_0^{\infty} \frac{u f_2^0(u)}{u^2 - \omega^2} du; \quad (4)$$

where Z is the atomic number and P indicates the Cauchy principal value of integrals.

Figure 3 shows the analyses of the (002) and (003) peak positions by using the calculated f_1^0 and Eq. (1). In the calculation, there is a large difference with finite δ , which indicates that the effects of refraction are substantial in these absorption edges. From panel (a) and (c), one can see that at the (002) peak (normal Bragg peak) the agreement between experiment and calculation is good, which confirms the validity of our analyses. However, panels (b) and (d) show that at the (003) peak (interface-sensitive peak) the agreement is rather poor. We believe that this is due to the electronic reconstruction of Ti 3d and O 2p states at the interface, which changes the optical properties from those of the pure components. Eq. (1) works well for the normal Bragg peak (002), which is not sensitive to the interfaces, but for the interface-sensitive peak (003), it does not provide a good description. This reveals that the underlying assumption of sharp interfaces is not appropriate and implies a different electronic structure and thereafter also a different energy-dependent dielectric constant from that assumed in Eq. (1). From our experimental results alone, we cannot exclude the possibility that this is due to the existence of oxygen vacancies or disorder effects at the interface. However, the good agreement of the (002) peak assuming an ideal structure points toward electronic reconstruction. Panel (e) shows that at the La 3d edge the (003) peak follows the calculation, which indicates that there is not a serious interdiffusion of La atoms [26] at the interface.

Next we analyzed the reflectivity spectra. The reflectivity can be simulated using the recursive Parratt's method [27, 28]. Here we considered four models as shown in Fig. 4 (g). Model A is the case where all

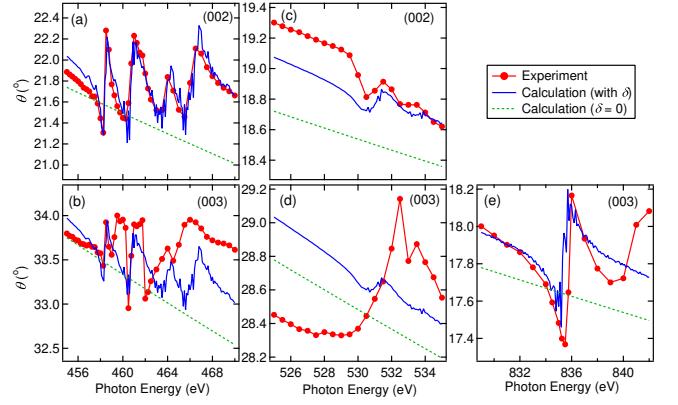


FIG. 3: (Color online) Peak-position analyses by considering the effects of refraction (δ). (a) (002) at the Ti 2p edge. (b) (003) at the Ti 2p edge. (c) (002) at the O 1s edge. (d) (003) at the O 1s edge. (e) (003) at the La 3d edge.

interfaces are sharp. Model C is the case without any sharp interfaces with or at the interface taken to be the average of that of STO and LAO. These two models are considered as "symmetric models" because they do not consider the difference of $\text{AlO}_2/\text{LaO}/\text{TiO}_2/\text{SrO}$ and $\text{TiO}_2/\text{SrO}/\text{AlO}_2/\text{LaO}$ interfaces. Asymmetric models are models B1 and B2. These models include different interfaces as far as electronic roughness is concerned. In model B1, only the latter interfaces are sharp and in model B2, only the former are sharp. It was previously reported that metallic behavior is only observed at the former interface [2] and also the former interfaces are atomically less sharp than the latter ones [4], seeming to support model B1. Motivated by these studies, we investigated which model can best describe the reflectivity spectra.

Figure 4 shows the comparison of the reflectivity spectra between experiment and calculation. From this figure one can see that the strong (003) peaks are not reproduced by models A and C, which demonstrates the necessity of the asymmetric models. In the two asymmetric models, model B1 reproduces the experimental results fairly well but for Ti 2p on-resonance, model B2 gives a better description of the experiment. Also we obtain the best fitting when the thickness of the interface (d) is taken to be about 3 uc. We should note here that in model A, with no reconstruction, the (003) peak is still present particularly at La on-resonance. This is due to the short penetration depth of the x-rays at resonance, providing in perfect extinction as described before. From these results, we conclude that our SL is a highly asymmetric system with two different types of interfaces, and the thickness of the interface is about 3 uc.

In summary, we investigated the electronic structures of the STO/LAO SL by resonant soft x-ray scattering.

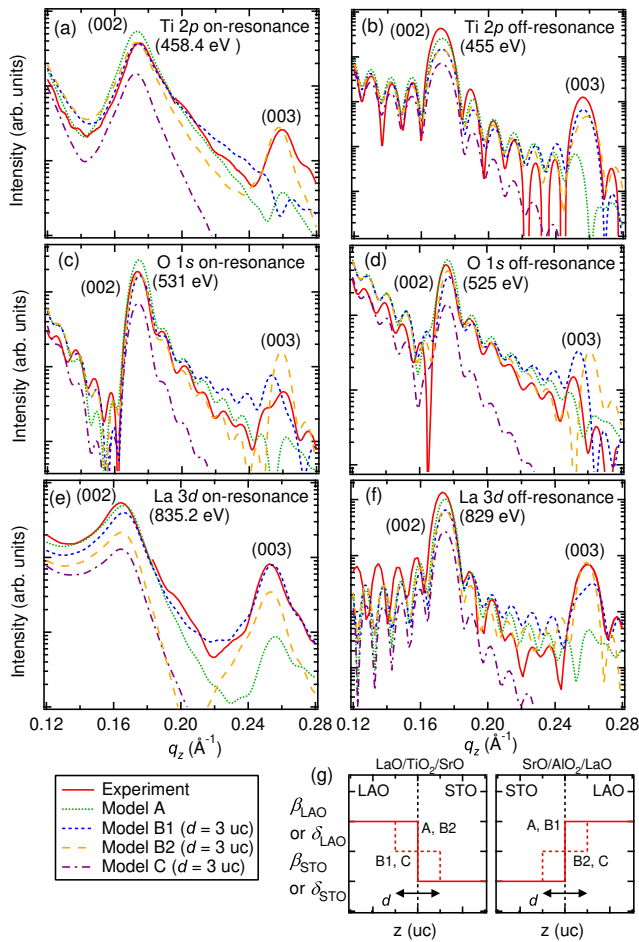


FIG. 4: (Color online) Comparison of the reactivity spectra between experiment and calculation. (a) Ti 2p on-resonance. (b) Ti 2p off-resonance. (c) O 1s on-resonance. (d) O 1s off-resonance. (e) La 3d on-resonance. (f) La 3d off-resonance. (g) Models of our superlattice samples.

From reactivity measurements, we observed oscillations due to superlattice structures. The forbidden (003) peak was observed even at off-resonance, in sharp contrast to the case of LM O / SM O [20]. Both (002) and (003) Bragg peaks show resonant enhancement at the Ti 2p, O 1s, and La 3d absorption edges. From the peak position analyses taking into account the effects of refraction, the behavior of (002) and (003) at the La 3d absorption could be reproduced by calculations but that of (003) at the Ti 2p and O 1s absorption edges could not be reproduced by the model which does not take into account changes in the atomic scattering factors due to electronic reconstruction. These results point to electronic reconstruction of Ti 3d and O 2p at the interface. From reactivity analyses, we found evidence for highly asymmetric properties of the STO/LAO SL, which means that the $\text{AlO}_2/\text{LaO}/\text{TiO}_2/\text{SrO}$ and the $\text{TiO}_2/\text{SrO}/\text{AlO}_2/\text{LaO}$ in-

terfaces are quite different. The thickness of the interface was determined to be about 3 uc.

The authors would like to thank I. Elmov and A. Fujimori for informative discussions. H.W. acknowledges financial support from the Japan Society for the Promotion of Science. J.G. acknowledges the support by DFG. C.S.-L. acknowledges the support by the DFG through SFB 608. This work was made possible by financial support from the Canadian funding Agencies NSERC, CRC, CIFAR, and CFI.

Electronic address: wadati@phas.ubc.ca

- [1] H. Yamada, Y. Ogawa, Y. Ishii, H. Sato, M. Kawasaki, H. Aoh, and Y. Tokura, *Science* 305, 646 (2004).
- [2] A. Ohtomo and H. Y. Hwang, *Nature* 427, 423 (2004).
- [3] N. Reyren, S. Thiel, A. D. Caviglia, L. F. Kourkoutis, G. Hammer, C. Richter, C. W. Schneider, T. Kopp, A. S. Ruetschi, D. Jaccard, M. Gabay, D. A. Muller, J.-M. Triscone, and J. Mannhart, *Science* 317, 1196 (2007).
- [4] N. Nakagawa, H. Y. Hwang, and D. A. Muller, *Nature Materials* 5, 204 (2006).
- [5] M. Huijben, G. Rijnders, D. H. A. Blank, S. Bals, S. V. Aert, J. Verbeeck, G. V. Tendeloo, A. Brinkman, and H. Hilgenkamp, *Nature Materials* 5, 556 (2006).
- [6] S. Thiel, G. Hammerl, A. Schmehl, C. W. Schneider, and J. Mannhart, *Science* 313, 1942 (2006).
- [7] A. Brinkman, M. Huijben, M. V. Zalk, J. Huijben, U. Zeitler, J. C. M. van, W. G. V. D. Wiel, G. Rijnders, D. H. A. Blank, and H. Hilgenkamp, *Nature Materials* 6, 493 (2007).
- [8] G. Herranz, M. Bascletic, M. Bibes, C. Carretero, E. Tafia, E. Jacquet, K. Bouzehouane, C. Deranlot, A. Hamzic, J.-M. Broto, A. Barthelmy, and A. Fert, *Phys. Rev. Lett.* 98, 216803 (2007).
- [9] W. Siemons, G. Koster, H. Yamamoto, W. A. Harrison, G. Lucovsky, T. H. Geballe, D. H. A. Blank, and M. R. Beasley, *Phys. Rev. Lett.* 98, 196802 (2007).
- [10] A. Kalabukhov, R. Gunnarsson, J. Borjesson, E. Olsson, T. Claesson, and D. Winkel, *Phys. Rev. B* 75, 121404 (R) (2007).
- [11] M. Bascletic, J.-L. Maurice, C. Carretero, G. Herranz, O. Copie, M. Bibes, E. Jacquet, K. Bouzehouane, S. Fusil, and A. Barthelmy, *Nature Materials* 7, 621 (2008).
- [12] R. Pentcheva and W. E. Pickett, *Phys. Rev. B* 74, 035112 (2006).
- [13] M. S. Park, S. H. Rhim, and A. J. Freeman, *Phys. Rev. B* 74, 205416 (2006).
- [14] R. Hesper, L. H. Tjeng, A. Heeres, and G. A. Sawatzky, *Phys. Rev. B* 62, 16046 (2000).
- [15] M. Takizawa, H. Wadati, K. Tanaka, M. Hashimoto, T. Yoshida, A. Fujimori, A. Chikamatsu, H. Kumigashira, M. Oshina, K. Shibuya, T. M. Ihara, T. Ohnishi, M. Lippmaa, M. Kawasaki, H. Koinuma, S. Okamoto, and A. J. Millis, *Phys. Rev. Lett.* 97, 057601 (2006).
- [16] Y. Hotta, H. Wadati, A. Fujimori, T. Susaki, and H. Y. Hwang, *Appl. Phys. Lett.* 89, 251916 (2006).
- [17] H. Wadati, Y. Hotta, A. Fujimori, T. Susaki, H. Y. Hwang, Y. Takata, K. Horiba, M. Matsunami, S. Shin, M. Yabashi, K. Tamasaki, Y. Nishino, and T. Ishikawa,

- Phys. Rev. B 77, 045122 (2008).
- [18] K. Yoshinatsu, R. Yasuhara, H. Kumigashira, and M. Oshima, Phys. Rev. Lett. 101, 026802 (2008).
- [19] P. Abbamonte, L. Venema, A. Rusydi, G. A. Sawatzky, G. Logvenov, and I. Bozovic, Science 297, 581 (2002).
- [20] S. Smadici, P. Abbamonte, A. Bhattacharya, X. Zhai, B. Jiang, A. Rusydi, J. N. Eckstein, S. D. Bader, and J. M. Zuo, Phys. Rev. Lett. 99, 196404 (2007).
- [21] S. Smadici, J. C. T. Lee, S. Wang, P. Abbamonte, A. Gozar, G. Logvenov, C. D. Cavellin, and I. Bozovic, arXiv:0805.3189v1.
- [22] M. Kawasaki, K. Takahashi, T. Maeda, R. Tsuchiya, M. Shinohara, O. Ishihara, T. Yonezawa, M. Yoshimoto, and H. Koinuma, Science 266, 1540 (1994).
- [23] J. Schlappa, C. Schuster-Langeheine, C. F. Chang, Z. Hu, E. Schierle, H. Ott, E. Weschke, G. Kaindl, M. Hüben, G. Rijnders, D. H. A. Blank, and L. H. Tjeng, arXiv:0804.2461v1.
- [24] D. Attwood, Soft X-Rays and Extreme Ultraviolet Radiation (Cambridge University Press, Cambridge, England, 1999).
- [25] B. L. Henke, E. M. Gullikson, and J. C. Davis, At. Data & Nucl. Data Tables 54, 181 (1993).
- [26] P. R. Willmott, S. A. Pauli, R. Herger, C. M. Schlepütz, D. Martocchia, B. D. Patterson, B. Delley, R. Clarke, D. Kumah, C. Cionca, and Y. Yacoby, Phys. Rev. Lett. 99, 155502 (2007).
- [27] L. G. Parratt, Phys. Rev. 95, 359 (1954).
- [28] J. H. Underwood and J. T. W. Barbee, Appl. Opt. 20, 3027 (1981).